# Nonlinear optical properties of $Er_2O_3$-doped $75Nb_2O_5$-$20TeO_2$-5ZnO glasses

**Yufei Wang (王宇飞)[1], Zhenrong Sun (孙真荣)[1], Shi'an Zhang (张诗按)[1], Zugeng Wang (王祖庚)[1], Jian Lin (林 健)[2], Wenhai Huang (黄文昆)[2], Zhizhan Xu (徐至展)[3], and Ruxin Li (李儒新)[3]**

[1]*Key Laboratory of Optical and Magnetic Resonance Spectroscopy, and Department of Physics, East China Normal University, Shanghai 200062*

[2]*School of Material Science and Engineering, Tongji University, Shanghai 200092*

[3]*Shanghai Institute of Optics and Fine Mechanics, Chinese Academy of Sciences, Shanghai 201800*

Received October 28, 2003

We have performed time-resolved degenerate four-wave mixing (DFWM) experiments in $75Nb_2O_5$-$20TeO_2$-5ZnO glasses doped by $Er_2O_3$ at different excitation intensities and lattice temperatures. DFWM signal exhibits three peaks at high excitation intensities, where a main peak appears at zero time delay and two rather weak side peaks locate symmetrically at the negative and positive time delay, respectively. The main peak is attributed to local-field effect and two side peaks are attributed to Coulomb interaction (CI).

*OCIS codes:* 190.4380, 320.7130, 160.4760, 190.0190.

Telluride glasses are very kind of promising materials for laser and nonlinear optical applications for their electrical and nonlinear optical properties, such as high nonlinear refractive index, wide infrared transmittance, low melting temperature, low phonon maxima and higher dielectric constants. Telluride glasses are regarded as perfect ultrafast optical switch materials for their high third-order nonlinear susceptibility[1−6]. Recently, telluride glasses with $Er_2O_3$ dopant have received more interests because $Er_2O_3$ can improve their optical nonlinearities. The researches indicate that $Er_2O_3$-doped telluride glasses may exhibit rather high second-, third- and even fifth-order nonlinear susceptibilities, their high refractive index may broaden the gain bandwidth, thus the $Er_2O_3$-doped telluride fiber amplifier is now a well-known competitive candidate for broadband optical amplifiers in optical communication[7−10]. For the potential use of the telluride glassy matrices in optical communication system, it is necessary to comprehend their nonlinear effect. In this letter, we investigate the line shape of degenerate four-wave mixing (DFWM) in $75Nb_2O_5$-$20TeO_2$-5ZnO glasses with $Er_2O_3$ dopant at different excitation intensities and lattice temperatures.

Appropriate mixtures of $TeO_2$, $Nb_2O_5$, ZnO and $Er_2O_3$ are melted in gold crucible for 25−30 minutes at 850−950 °C, and quenched to room temperature in steel mold and annealed at 300−350 °C for 2−4 hours. The intact glass is picked out and its surface is polished for the following measurement. The concentration of $Er^{3+}$ is 0.1%, 0.25% and 0.5%, respectively.

Experimental setup for time-resolved four-wave mixing (FWM) experiments is shown in Fig. 1. The laser beam, from Spitfire Regenerative Amplifier with the central wavelength of 800 nm and the repetition rate of 1 kHz, is split into two linearly parallel polarized beams, one beam as probing is delayed by $T$ with respect to another beam as pumping, and then the two split beams spatially overlap on the sample. The coherent wave packet created by pumping beam leaves a macroscopic-dipole moment with a corresponding first-order polarization $p^{(1)}$, which is converted to a grating by the second beam, part of the second beam is then diffracted at this grating and yields a third-order polarization $p^{(3)}$, and radiated in the direction $k_3 = 2k_2 - k_1$[11].

Transient coherent spectroscopy has been increasingly used to investigate the properties of and the interactions among various elementary excitations in semiconductors. In the two-pulse self-diffracted FWM experiment, the two pulses create a transient grating and the

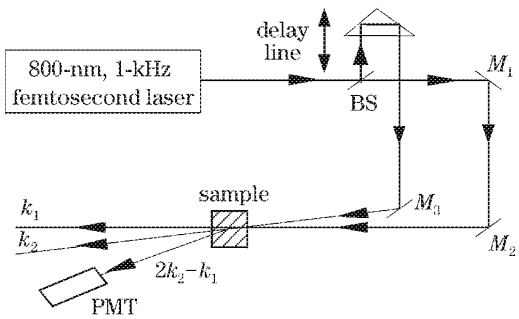


Fig. 1. Experimental setup for DFWM measurements, where BS is beam splitter, $M_1$, $M_2$ and $M_3$ are the reflective mirrors, PMT is photomultiplier tube.

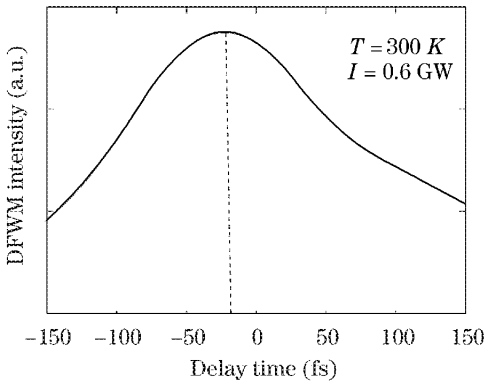


Fig. 2. DFWM signal with the delay time $T$ at the temperature of 300 K and the intensity of 0.6 GW.

diffracted signal is measured in a background-free direction. Considerable information about atoms, molecules, and solids has been obtained by such measurements[12].

The DFWM signal of $75Nb_2O_5$-$20TeO_2$-5ZnO glasses with 0.1% $Er_2O_3$ is shown at room temperature and low excitation intensity, it exhibits an ensemble of homogeneously broadened line shape (as shown in Fig. 2). In a two-level system, when the laser pulse width is proximate to the transverse relaxation time $T_2$, the correlation signal is the convolution of the laser pulse with unhomogeneously and homogeneously broadened systems. After the first laser pulse passes the resonant or near-resonant absorption medium, the related particles (atom, ion or molecule) are stimulated to the excited state, and move at the same phase, then relax as the time evolves. If the second pulse arrives before the excited states relax and dephase, then it interferes with the memory field, which is formed by the interaction between the excited states and the first laser pulse, and a grating will be formed. The character of the grating is the same as that of the grating which is formed when the two pulses arrive at the medium together, only the amplitude of the grating weakens as the time postpones. The interaction between electrons and holes in the presence of an external field is somewhat analogous to a paramagnet or a dense dielectric medium, which is related to the local-field effects. For the homogeneously broadened systems, the intensity of the DFWM signal in a dense system consisting of two-level atoms with local-field correction, one finds[13]

$$\delta P_{k_3}^{(3),\mathrm{hom}}(t) = \kappa \mathrm{e}^{-i\Omega(t-2T)-\gamma_2 t}\{\Theta(T)\Theta(t-T) + i(2V/\gamma_1)[\Theta(T)\Theta(t-T)(1-\mathrm{e}^{-\gamma_1(t-T)}) + \Theta(-T)\Theta(t)(1-\mathrm{e}^{-\gamma_1 t})\mathrm{e}^{2\gamma_2 T}]\}, \quad (1)$$

where $\kappa = -iN|\mu|^4 E^2 \delta E^*$ and $\Theta$ is the Heaviside step function, $V = N|\mu^2|L$, $N$ is the density of atoms, $L$ is the Lorentz local field factor, $\gamma_1 = 1/T_1$ and $\gamma_2 = 1/T_2$ are the longitudinal and transverse relaxation rates, respectively. The first term is the usual one for non-interacting two-level atoms, which contributes for positive time delay only [proportional to $\Theta(T)$]. The two other terms (proportional to $V$) are due to the local-field correction. The first one [proportional to $\Theta(T)$] also contributes at positive time delay, whereas the other [proportional to $\Theta(-T)$] contributes only at negative time delay. It is interesting to note that the three terms are orthogonal. The first one is orthogonal in the complex plane to the two others, which are orthogonal to one another in time. Thus, the three contributions do not interfere, the time-integrated diffracted signal is

$$I_{k_3}^{\mathrm{hom}}(T) \propto \Theta(T)\mathrm{e}^{-2\gamma_2 T} + \frac{4V^2}{(2\gamma_2+\gamma_1)(\gamma_2+\gamma_1)} \times [\Theta(T)\mathrm{e}^{-2\gamma_2 T} + \Theta(-T)\mathrm{e}^{4\gamma_2 T}]. \quad (2)$$

Here we can see that the signal exhibits a finite rise time with a time constant $T_2/4$ and a decay with a time constant $T_2/2$, which is similar to the case of Coulomb interactions between excitons[14,15]. So, it is easy to interpret the results intuitively. With or without local-field interaction, a grating is formed once both pumping pulse and probing pulse (for either time ordering) have arrived in the sample. Without local-field interaction only the applied fields can diffract from this grating. If probing pulse comes first (negative time delay), the grating is only set up after pumping pulse arrives, no photon from probing pulse is available since pumping pulse has already passed the sample. Thus no signal in the direction $2k_2 - k_1$ is generated for negative time delay. With local-field interaction, however it is possible to diffract the leftover of the first-order polarization induced by pumping off the grating formed as soon as pumping pulse arrives. Since two first-order polarizations from probing pulse are involved in this process and both decay with a time constant $T$ until probing pulse arrives, the signal decays with twice the time constants for negative time delay. In addition, Yajima and Taira[16] predict that this diffracted signal due to coherent polarization interactions rises as $\sim \exp(4T/T_2)$ for $T < 0$ and decays as $\sim \exp(-2T/T_2)$ for $T > 0$, where $T$ is the delay time between the two laser pulses, $T_2$ is the polarization dephasing time. The temporal evolution of DFWM signal may yield information about the phase relaxation processes and the nature of the excited states. In the past time, the time-resolved FWM experiments on semiconductors have been used to determine the dephasing of excitons[17–19], free electrons and holes[20]. These studies have been concentrated on the decay of the diffracted signal at positive delays. Meanwhile, the signals are asymmetric in time and consist of exponentially rising and decaying wings. The asymmetric beating is due to the excitonic non-uniform splitting and a many-level superposition of the Wannier-Stark (WS) states, as the spectrum of the excitation laser pulse covers several of these states[21].

Figure 3 shows DFWM signal for the different excitation laser intensities at the room temperature. With the excitation intensity increasing, the main peak at zero time delay strengthens less pronounced and the position of the peak inclines to the negative time delay. In addition, there are two additional side band signals not only at the negative time delay but also at the positive time delay far away from the zero time delay, they gradually strengthen as the excitation intensity increasing. The positions of the two peaks are independent of the pulse duration, temperature and excitation intensity, but the

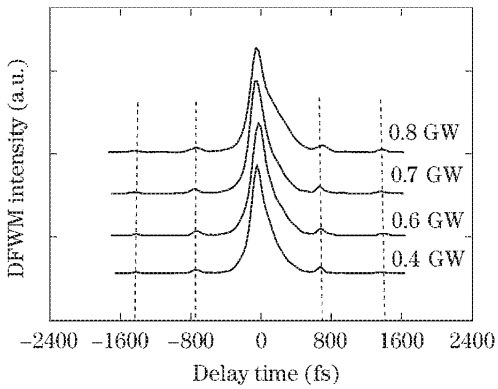


Fig. 3. The DFWM signal for the different excitation laser intensities at the temperature of 300 K.

values of the maximum depend on the temperature and excitation intensity. In this letter, the negative time delay side band signal has been explained by many-body effects: excitons in the sample are not isolated two-level systems, and interact by the many-body Coulomb interaction (CI). If probing pulse arrives before pumping pulse (negative delay time), there are photons of probing pulse left when the grating is formed and diffracted in direction $2k_2 - k_1$. It has been shown in Eq. (2) that this signal rises with $T_2/4$. This result has been confirmed by the previous experiment for coherent polarization interaction on time-resolved DFWM in semiconductors. So the delayed rise can be unambiguously attributed to Coulomb-mediated many-body effects[22−24]. Whereas strong CI between excitons leads to the evolution of a polarization wave with a time delay in the order of the phase relaxation time $T_2$[25]. For the positive time delay side band signal, pumping pulse arrives before probing pulse, the pumping pulse with wave vector $k_1$ creates a macroscopic polarization which decays with the dephasing time $T_2$. The probing pulse with wave vector $k_2$ will form a grating with the polarization left from the pumping pulse. The part of the pumping pulse can then be diffracted from this grating into the direction $2k_2 - k_1$. Then the signal is completely dominated by the delayed peak, which results from exciton-exciton interaction and is modulated due to the interference between the different Wannier-Stark (WS) excitons[26] .

Figure 4 shows the time-integrated diffracted DFWM signal versus time delay $T$ for the different lattice temperature at 0.8 GW. The signals are asymmetric in time and consist of exponentially rising and decaying wings. With lattice temperature increasing, the two additional side band signals at negative and positive time delay get stronger, whereas the zero time delay signal demonstrates less pronounced. In addition, both the decay and rise time get shorter, ruling out the pulse profile as determining either of them. At low temperatures, the thermal phonon contribution to the dephasing is small, the decay time is found twice larger than the corresponding rise time. With lattice temperature increasing, both time constants decrease. Similar behavior is observed as $T_2$ is decreased with the excitation laser intensity increasing. In addition, we observe that FWM peaks at $10-15$ times of the pulse width at 7 K, the peak position and the rise time are not related to pulse width or $T$. A comparison of the peak position and delay constant $T$ shows that the signal peaks roughly locate at $2T$ or close to $T_2$. Moreover, a small side band peak appears near to the zero time delay. The origin of the shifts of the signal maximum is considered because biexciton resonance and biexciton process mainly contribute to the higher-order nonlinear responses[27].

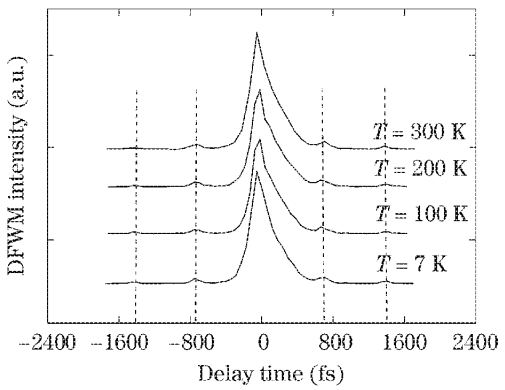


Fig. 4. The diffracted DFWM signal for four different temperature at 0.8 GW.

We have demonstrated the coherent polarization interactions and nonlinear optical effects in time-resolved FWM experiments at the different excitation intensities and lattice temperatures. For different excitation intensities and lattice temperatures, the polarization dephasing time $T_2$ is generally invariable due to low phonon energy in telluride glass. At high excitation laser intensity or lattice temperature, the zero time delay signal strengthens, which is attributed to "local-field effect". Furthermore, a nonlinear response is observed, two additional time-dependent signals far away from zero time delay gradually strengthen with increasing excitation intensity or lattice temperature, which are due to the Coulomb interaction.

This work was supported by Shanghai Priority Academic Discipline, the National Natural Science Foundation of China (No. 10234030 and 10074015), the National Key Project for Basic Research (No. 1999075204), the Project Sponsored by Shanghai Science and Technology Committee, and the Key Project Sponsored by National Education Ministry of China. Z. Sun is the author to whom the correspondence should be addressed, his e-mail address is zrsun@public4.sta.net.cn.

## References

1. S.-H. Kim, T. Yoko, and S. Sakka, J. Am. Ceram. Soc. **76,** 2486 (1993).
2. Y. Kowada, K. Morimoto, H. Adachi, M. Tatsumisago, and T. Minami, J. Non-Cryst. Solids **196,** 204 (1996).
3. A. K. Yakhend, J. Am. Ceram. Soc. **49,** 670 (1996).
4. H. Nasu, O. Matsushita, K. Kamiya, H. Kobayashi, and K. Kubodera, J. Non-Cryst. Solids **124,** 275 (1990).
5. G. V. Prakash, D. N. Rao, and A. K. Bhatnagar, Solid State Commun. **119,** 39 (2001).
6. A. Berthereau, E. Fargin, A. Villezusanne, R. Olazcuaga, G. Le Flem, and L. Ducasse, J. Solid State Chem. **126,** 143 (1996).
7. Y. G. Choi, K. H. Kim, S. H. Park, and J. Heo, J. Appl. Phys. **88,** 3832 (2000).
8. A. Mori, Y. Ohishi, and S. Sudo, Electron. Lett. **33,** 863 (1997).
9. Y. Ohishi, A. Mori, M. Yamada, H. Ono, Y. Nishida, and K. Oikawa, Opt. Lett. **23,** 274 (1998).
10. T. Nakai, Y. Noda, T. Tani, Y. Mimura, T. Sudo, and S. Ohno, OSA Tops. **25,** 82 (1998).
11. P. Leisching, W. Beck, H. Kurz, K. Kohler, W. Schafer, and K. Leo, Solid State Electron. **40,** 545 (1996).
12. D. S. Kim, J. Shah, and T. C. Damen, Phys. Rev. Lett. **69,** 2725 (1992).
13. M. Wegener, D. S. Chemla, S. Schmitt-Rink, and W. Schafer, Phys. Rev. A **42,** 5675 (1990).
14. C. Stafford, S. Schmitt-Rink, and W. Schafer, Phys. Rev. B **41,** 10000 (1990).

15. K. Leo, M. Wegener, J. Shah, D. S. Chemla, E. O. Gobel, T. C. Damen, S. Schmitt-Rink, and W. Schafer, Phys. Rev. Lett. **65,** 1340 (1990).
16. Yajima and Y. Taira, J. Phys. Soc. Jpn. **47,** 1620 (1979).
17. L. Schultheis, M. D. Sturge, and J. Hegarty, Appl. Phys. Lett. **47,** 995 (1985).
18. L. Schultheis, J. Kuhl, A. Honold, and C. W. Tu, Phys. Rev. Lett. **57,** 1635 (1986).
19. A. Honold, L. Schultheis, J. Kuhl, and C. W. Tu, Phys. Rev. B **40,** 6442 (1989).
20. P. C. Becker, H. L. Fragnito, C. H. B. Cruz, R. L. Fork, J. E. Cunningham, J. E. Henry, and C. V. Shank, Phys. Rev. Lett. **61,** 1647 (1988).
21. P. Leisching, P. H. Bolivar, W. Beck, Y. Dhaibi, F. Bruggemann, R. Schwedler, and H. Kurz, Phys. Rev. B **50,** 14389 (1994).
22. Weiss, M. A. Mycok, J.-Y. Bigot, S. Schmitt-Rink, and D. S. Chemia, Phys. Rev. Lett. **69,** 2685 (1992).
23. W. Schafer, F. Jahnko, and S. Schmitt-Rink, Phys. Rev. B **47,** 1217 (1993).
24. W. Schafer, in *Optics in Semiconductor Nanostructures* F. Henneberger, S. Schmitt-Rink, and E. O. Gobel (ed.) (Akademie Verlag, Berlin, 1993) and references therein.
25. K. Leo, E. O. Gobel, T. C. Damen, J. Shah, S. Schmitt-Rink, W. Schafer, J. F. Muller, K. Kohler, and P. Ganser, Phys. Rev. B **44,** 5726 (1991).
26. P. Leisching, W. Beck, and H. Kurz, Phys. Rev. B **51,** 7962 (1995).
27. K. Akiyama, N. Tomita, Y. Nomura, and Toshiiroisu, Physica B **272,** 505 (1999).